Comparative Analysis of Simplified and Finite Element Method Approaches for Seismic Forces in Circular Tunnels

A. Achouri[1] and M. N. Amrane[2]
[1]*Department of Mechanical Engineering, USTHB University, Algiers, Algeria*
[2]*Department of Mechanical Engineering, BISKRA University, Biskra, Algeria*
E-mail: abderrahim.achouri@usthb.edu.dz

ABSTRACT: This paper presents a comparative analysis between simplified and Finite Element Method (FEM) approaches for evaluating seismic forces in circular tunnels, with a specific focus on the Algiers Metro as a practical case study, considering the Boumerdes earthquake in 2003. The FE modeling was carried out under plane strain conditions, using the contraction method to phase the performed model and incorporating the Volume Loss coefficient (VL). The behavior of soil and tunnel elements was considered linear elastic. Based on the maximum strain rate of the soil medium, various simplified approaches existing in the literature were adopted in this study, including solutions proposed by Wang (1993), Penzien (2000), Bobet (2003, 2010), and Park et al. (2009). The maximum shear strain rate was determined by plotting the cumulative horizontal displacement of the soil profile and then using this value to deduce the vertical strain rate. Results indicate that increasing VL values initially reduce axial thrust, followed by an increase. Shear force and bending moment proportionally increased with the VL ratio, remaining within the practical range of simplified solutions. The best agreement between the simplified and FEM approaches was observed when VL ranged between 1 and 2. Additionally, the total principal stresses around the tunnel increased with the VL ratio. This study highlights the importance of estimating the appropriate maximum strain rate and VL ratio to achieve accurate results while using both simplified and FEM approaches.

KEYWORDS: Seismic Forces, Circular Tunnels, Simplified Approaches, FE Modeling, and Volume Loss Coefficient.

1. INTRODUCTION

Tunnels have become one of the most important components of infrastructure systems, as they play an important role in transportation networks and measure the extent of development and urbanization in the world's major cities. Tunnels are among the most secure structures in civil engineering. However, numerous significant damages, such as fissures and collapses, have been surveyed and reported worldwide in recent decades. High-magnitude forces include earthquakes (e.g., the 1995 Kobe, Japan earthquake, the 1999 Chi-Chi, Taiwan earthquake, the 2003 Boumerdes (Algeria) earthquake, and the 2023 Kahramanmaras, Turkey earthquake) that caused the majority of these damages. For this reason, studies on developing tunnel designs that are more resistant to seismic events have become very important. For the design and construction of tunnels, seismic analysis is based on analytical solutions, numerical analyses, and experimental studies. Identifying internal forces and deformations through analytical and experimental studies is difficult because it depends on various factors such as adopted simplifications, data availability, and the accuracy of used equipment. Several analytical solutions for the cross-section of a tunnel have been developed to calculate the internal seismic forces of tunnel linings (Höeg, 1968; Peck et al., 1972; J. N. Wang, 1993; Penzien and Wu, 1998; Penzien, 2000; A Bobet, 2003; Corigliano, 2007; Park et al., 2009; Antonio Bobet, 2010). These analytical formulations are primarily based on the kinematic soil-structure interaction and the relative stiffness method. However, various conditions and assumptions, such as the elastic responses of the soil and tunnel, seismic loading simulation in semi-static construction, full-slip and no-slip conditions, and others, are also considered. Tunnel seismic analysis is complex because it involves several factors, such as seismic wave characteristics, regional geology, geometry, and the behaviors of ground and tunnel materials. Due to this complexity, numerous advanced software codes based on numerical methods such as the Finite Element Method (FEM), Finite Volume Method (FVM), and Finite Difference Method (FDM) have been developed in recent years (Hashash et al., 2005; Corigliano et al., 2011; Sandoval and Bobet, 2017; Singh et al., 2017; Salemi et al., 2018; Sandoval and Bobet, 2020). Additionally, accurately determining soil properties, such as stiffness and strength, with accuracy is one of the main issues in numerical analysis. These characteristics are obtained by combining the findings of various laboratory and field tests (Surarak et al., 2012; Likitlersuang et al., 2013a; Likitlersuang et al., 2013b; Likitlersuang et al., 2018; Sukkarak et al., 2021a). Along with analytical and numerical methods, researchers have used experimental studies to understand better how tunnels react during earthquakes and to develop approaches for building seismically resistant tunnels. Seismic analysis experimental investigations generally involve subjecting physical models of tunnels to various types of seismic stresses and evaluating the resulting response using common experimental methods such as shake table testing, centrifuge testing, and field testing (Bilotta et al., 2009; Chen et al., 2010; Lanzano et al., 2015; Tsinidis et al., 2020; Zhang et al., 2022). In recent years, several numerical studies have shed light on various aspects of tunneling, including examining settlements induced by tunneling, interactions between twin tunnels, and the impacts of adjacent excavations on existing structures. These studies demonstrate how numerical methods can optimize tunnel design, for example, by minimizing settlements and optimizing the spacing of twin tunnels, as well as improving construction practices to protect nearby structures. The results highlight the important role of numerical modeling in predicting and mitigating risks associated with tunneling activities, thereby ensuring the safety and stability of new and existing underground infrastructure (Likitlersuang et al., 2014; Govindasamy et al., 2020; Muenpetch et al., 2023; Phutthananon et al., 2023). The tunnel-soil interaction phenomenon, an important part of the seismic analysis, can significantly influence the seismic responses and performance of tunnels, including changes in seismic force distribution, deformation and stress in the tunnel lining and supports, and the potential for damage. According to the literature, the presence of a tunnel leads to the amplification of seismic waves on the overground, with the maximum amplification occurring at the tunnel-soil interface, particularly at short frequencies. Additionally, reducing the tunnel depth results in a more intense ground seismic response and greater seismic amplification. The presence of a soft soil layer generally increases internal forces and deformations, especially when a very soft soil layer intersects a flexible tunnel at the springline. (Asheghabadi and Matinmanesh, 2011; Sun et al., 2020; Alielahi and Feizi, 2021). The tunnel-soil-interface interaction is significant as a full-slip interface results in a higher bending moment in the tunnel compared to a no-slip condition (Choudhury et al., 2019). These effects must be considered during tunnel design and construction, as well as seismic performance evaluation and the

development of mitigation strategies to reduce the risk of damage and collapse during earthquakes (Jaw-Nan Wang and Munfakh, 2001). Other dynamic impacts, such as traffic and blast loads, should not be overlooked in these strategies (Achouri and Amrane, 2020; Achouri and Amrane, 2021; Cheng et al., 2021). This study numerically investigates the seismic behavior of internal forces in the Algiers Metro Project tunnel (extended line 1) due to the horizontal and vertical components of the 2003 Boumerdes earthquake. The soil and tunnel elements' behavior are described using the elastic constitutive model. Additionally, the study investigated the efficacy of incorporating the maximum vertical strain rate into existing simplified approaches to calculate internal forces under the impact of the vertical seismic component, comparing the results with those obtained through FE analysis (FEA).

2. FINITE ELEMENT ANALYSIS

Under plane strain conditions, a numerical modeling study was conducted using the FE software Plaxis2D. The case study involved a 2D geometric model with 15-node triangular elements for the soil and 5-node beam elements for the tunnel. The soil-tunnel interaction contacts were modeled as fully rigid. According to Kuhlemeyer and Lysmer (1973), the average element size (AES) condition was considered in the mesh generation procedure, ensuring it did not exceed $\lambda/8 = V_S/8f_{max}$. Here, λ represents the wavelength corresponding to the maximum frequency f_{max} of interest, and V_S is the shear wave of the medium. Rayleigh damping was assumed in this study where the damping matrix **C** is determined as a linear relationship between the mass **M** and stiffness **K** matrices:

$$\mathbf{C} = \alpha_R \mathbf{M} + \beta_R \mathbf{K} \tag{1}$$

The Rayleigh coefficients α_R and β_R can be estimated as:

$$\alpha_R + \beta_R \omega_{ni} = 2\omega_{ni}\xi \tag{2}$$

In this context, ξ represents the assumed damping ratio, and ω_{ni} denotes two circular natural frequencies of the elements under study. For this study, ω_1 is considered as the fundamental circular frequency of the site (SF), and ω_2 is set equal to 5SF (Kwok et al., 2007).

To ensure a low numerical damping and stable solutions, this study adopts the Newmark coefficients $\alpha_N = 0.3025$ and $\beta_N = 0.6$. Other combinations are also viable (Hilber et al., 1977; Brinkgreve, 2003).

To mitigate the rise in shear and normal stress components at the boundary, the viscous boundary approach proposed by Lysmer and Kuhlemeyer (1969) was applied, using the relaxation coefficients a = 1 and b = 0.25. These values are deemed effective in absorbing boundary waves (Brinkgreve, 2003).

Based on the contraction method proposed by Vermeer and Brinkgreve (1993), for computing ground movement due to tunneling, the 2D modeling was phased as follows:

- Phase 1 (initial stage): Only initial stresses are generated during this stage. Other than the soil domain, all components remained inactive.
- Phase 2 (construction stage): During this phase, tunnel liner components are activated while soil cluster elements within the liner are deactivated.
- Phase 3 (construction stage): The tunnel lining is contracted to simulate volume loss. The contraction rate was set at 0% to 3%.
- Phase 4 (dynamic stage): The boundaries are handled as viscous absorbent boundaries during this stage, and the associated constants are defined. Furthermore, earthquake loading time histories are applied along the model's base.

3. SIMPLIFIED APPROACHES

Wang's solution (1993) is employed as the initial interactive analytical approach for comparison with the FEA results. This approach is based on the compression and flexibility ratios (C, F) proposed by Peck et al. (1972) to evaluate the tunnel rigidity relative to the surrounding soil. Equations (3) and (4) evaluate the tensile and bending rigidity relative to the lining, respectively.

$$C = \frac{E_m(1-\nu_l^2)r}{E_l t(1+\nu_m)(1-2\nu_m)} \tag{3}$$

$$F = \frac{E_m(1-\nu_l^2)r^3}{6E_l I(1+\nu_m)} \tag{4}$$

Here, I represents the moment of inertia of the tunnel lining per unit width. E_m and ν_m denote the Poisson's coefficient and elasticity modulus of the medium. r, t and ν_l are the radius, thickness and Poisson's coefficient of the tunnel lining, respectively.

Assuming no-slip conditions, the axial thrust and bending moment can be expressed as follows:

$$T(\theta) = K_2 \frac{E_m}{(1+\nu_m)} r\gamma_{max} \cos 2\left(\theta + \frac{\pi}{4}\right) \tag{5}$$

$$M(\theta) = \frac{1}{6} K_1 \frac{E_m}{(1+\nu_m)} r\gamma_{max} cos 2\left(\theta + \frac{\pi}{4}\right) \tag{6}$$

Here, K_1 and K_2 are Wang's coefficients, and γ_{max} is the far-field shear strain. The coefficients are defined as follows:

$$K_1 = \frac{12(1-\nu_m)}{2F+5-6\nu_m} \tag{7}$$

$$K_2 = 1 + \frac{F[(1-2\nu_m)-(1-2\nu_m)C]-\frac{1}{2}(1-2\nu_m)^2+2}{F[(3-2\nu_m)+(1-2\nu_m)C]+C\left[\frac{5}{2}-8\nu_m+6\nu_m^2\right]+6-8\nu_m} \tag{8}$$

Penzien (2000) presented an analytical method for evaluating the axial force, shear force, and bending moment in the tunnel lining due to ovaling deflection under no-slip conditions as follows:

$$T(\theta) = -\frac{12E_l I R\gamma_{max}}{d^2(1-\nu_l^2)} \cos 2\left(\theta + \frac{\pi}{4}\right) \tag{9}$$

$$M(\theta) = -\frac{3E_l I R\gamma_{max}}{d(1-\nu_l^2)} \cos 2\left(\theta + \frac{\pi}{4}\right) \tag{10}$$

$$V(\theta) = -\frac{12E_l I R\gamma_{max}}{d^2(1-\nu_l^2)} \sin 2\left(\theta + \frac{\pi}{4}\right) \tag{11}$$

Penzien's coefficients are:

$$R = \pm\frac{4(1-\nu_m)}{(\alpha+1)} \tag{12}$$

$$\alpha = -\frac{24E_l I(3-4\nu_m)}{d^3 G_m(1-\nu_l^2)} \tag{13}$$

In the following, the presented relationships in the analytical solution of Park *et al.* (2009) are discussed for circular tunnels due to ovaling deformation under no-slip conditions:

$$\frac{T(\theta)}{G_s\gamma_c R} = -\frac{4(1-\nu_s)}{\Delta'}\left\{F + \left(\frac{1}{2} - \nu_s\right)C + 2\right\} \cos 2\left(\theta + \frac{\pi}{4}\right) \tag{14}$$

$$\frac{T(\theta)}{G_s\gamma_c R^2} = -\frac{4(1-\nu_s)}{\Delta'}\left\{1 + \left(\frac{1}{2} - \nu_s\right)C\right\} \cos 2\left(\theta + \frac{\pi}{4}\right) \tag{15}$$

With:

$$\Delta' = F[(3-2\nu_s)+(1-2\nu_s)C] + C\left[\frac{5}{2} - 8\nu_s + 6\nu_s^2\right] + 6 - 8\nu_s \tag{16}$$

where, ν_s and G_s denote the shear modulus and Poisson's coefficient of the soil around the tunnel, γ_c is the mean free-field shear strain, and Δ' is the coefficient of coverage response under no-slip conditions.

Based on the vertical and horizontal stresses (σ_v and σ_h) and the no-slip conditions, Bobet (2003) presented an analytical solution for calculating the axial force and bending moment as follows:

$$T(\theta) = \frac{\sigma_v+\sigma_h}{2}(1 + C_1)r_0 + \frac{\sigma_v-\sigma_h}{2}(1 - C_3)r_0 cos(2\theta) \quad (17)$$

$$M(\theta) = \frac{\sigma_v-\sigma_h}{2}(1 + C_2 + C_3)r_0^2 cos(2\theta) \quad (18)$$

Bobet's coefficients can be calculated as follows:

$$C_1 = \frac{1-2\nu-(1-\nu)C+(1-2\nu)\frac{C}{F}}{1+(1-\nu)C+\frac{C}{F}} \quad (19)$$

$$C_2 = -2\frac{(1-\nu)^2C+(1-\nu)-[(1-\nu)C+4]\frac{3}{F}}{(1-\nu)^2C+(1-\nu)(3-2\nu)+[(1-\nu)(5-6\nu)C+4(3-4\nu)]\frac{3}{F}} \quad (20)$$

$$C_3 = \frac{1}{3}\frac{(1-\nu)C-2-C_2[(1-\nu)C+4\nu]}{(1-\nu)C+2} \quad (21)$$

With:

$$C = \frac{E(1-\nu_s^2)r_0}{E_s A_s(1-\nu^2)} \quad (22)$$

$$F = \frac{E(1-\nu_s^2)r_0^3}{E_s I_s(1-\nu^2)} \quad (23)$$

For P-waves pressure:

$$\sigma_v = \frac{(1-\nu)E}{(1+\nu)(1-2\nu)}\varepsilon_v \quad (24)$$

$$\sigma_h = \frac{\nu}{(1-\nu)}\sigma_v \quad (25)$$

$$\varepsilon_v = \frac{V_{max}}{V_P} \quad (26)$$

ε_v , V_{max} and V_P are the far-field vertical strain, the peak ground velocity, and the ground pressure wave velocity, respectively.
For S-waves pressure:

$$\sigma_v = \frac{E}{2(1+\nu)}\gamma_{max} \quad (27)$$

$$\sigma_h = -\sigma_v \quad (28)$$

$$\gamma_{max} = \frac{V_{max}}{V_s} \quad (29)$$

where, γ_{max} and V_s represent the far-field shear strain and the ground shear wave velocity.

Bobet (2010) proposed another analytical solution under the no-slip conditions for determining *T* and *M* as follows:

$$T(\theta) = -(1 - C_2)G_m\gamma_{max}rsin(2\theta) \quad (30)$$

$$M(\theta) = -\frac{1}{2}(1 + C_1 + C_2)G_m\gamma_{max}r^2 sin(2\theta) \quad (31)$$

With:

$$C_1 = -2\frac{(1-2\nu_m)^2C'+(1-2\nu_m)-[(1-2\nu_m)C'+4]\frac{3}{F'}}{(1-\nu_m^2)C'+(1-\nu_m)(3-2\nu_m)+[(1-\nu_m)(5-6\nu_m)C'+4(3-4\nu_m)]\frac{3}{F'}} \quad (32)$$

$$C_2 = \frac{1}{3}\frac{(1-\nu_m)C'-2-C_1[(1-\nu_m)C'+4\nu_m]}{(1-\nu_m)C'+2} \quad (33)$$

$$C' = \frac{E_m r(1-\nu_l^2)}{E_l A(1-\nu_m^2)} \quad (34)$$

$$F' = \frac{E_m r^3(1-\nu_l^2)}{E_l I_l(1-\nu_m^2)} \quad (35)$$

Here, C_1, C_2, C', and F' denote Bobet's coefficients.

4. CHARACTERISTICS OF SEISMIC ACTIVITY AND REGIONAL ANALYSIS

On May 21, 2003, at 18:44 UTC (19:44 local time), a powerful earthquake hit northern Algeria, according to the Algerian Center of Research in Astronomy, Astrophysics, and Geophysics (CRAAG). This event was classified as a shallow earthquake with a magnitude of M_w = 6.8 and a focal depth of about 10 kilometers. CRAAG identified the epicenter offshore at 3.58°E and 36.91°N, close to Zemmouri village and about 50 kilometers from Algiers, where a strong motion duration of about 10 seconds was registered. A seismic moment of $M_0 = 2.4\times10^9$ Nm was estimated by the US Geological Survey (USGS). The maximum PGA recorded during the earthquake reached 0.58 g at 20 km from the epicenter and around 0.02 g up to 250 km. The region of Boumerdes–Algiers in Algeria, which is part of the Tell Atlas Mountains, constitutes a peri-Mediterranean section of the plate boundary along with the Rif Mountains in Morocco and the Betic Cordillera in Spain (Figure 1). This boundary is a result of the converging movement between the African and Eurasian tectonic plates, moving at a speed of approximately 4–6 mm annually. Seismic activities in the region encompass both thrust and strike-slip occurrences, indicating alterations in fault orientation and segmentation. Aftershocks tend to cluster close to the primary rupture plane, showcasing varied slip and segmentation influenced by geological irregularities and structural intricacies. The seismic event on May 21, 2003, led to an uplift of the coastline by 55 cm, underscoring notable thrust faulting and causing extensive destruction, including liquefaction. Evaluations of liquefaction susceptibility in Boumerdes and neighboring areas unveiled heightened vulnerability in specific locations. Despite Boumerdes having a generally low liquefaction susceptibility, certain zones, particularly in the vicinity of the Corso waterway, exhibit up to a 30% chance of liquefaction despite a safety margin above one. Furthermore, the topographic amplification due to gradual inclines resulted in severe harm to Corso. Data from the Boumerdes station within the epicentral zone, along with the Dar el Beida and Hussein Dey stations situated 29 km and 36 km away from the epicenter, respectively, indicates that the observed destruction in these areas can be attributed to site-specific impacts, notably the influence of high soil modes. Nevertheless, nonlinear soil impacts did not hold significant importance for numerous stations, and no direct correlation between site effects and structural damage was identified. The Boumerdes earthquake is significant in comprehending reverse faulting occurrences along the San Andreas fault system in the Los Angeles basin, owing to comparable transpressional tectonic settings and shortening rates. Similarities are observed between the 1980 El Asnam earthquake in Algeria and several earthquakes in California (1983 Coalinga, 1984 Kettleman Hills, and 1987 Whittier Narrows earthquakes), all taking place beneath actively developing folds. The 1994 Northridge earthquake, a common blind thrust incident in the northern Los Angeles basin, also displays these features. Given its relatively large magnitude, availability of geophysical data, and prompt response capability, the Boumerdes earthquake is exceptionally valuable for examining post-seismic deformation in a transpressional environment (Mahsas et al., 2008). Studies on the seismic characteristics of Northern Algeria and Northern Thailand indicate similarities that impact their assessments of hazard risk. These evaluations take into account variables like ground motion characteristics, attenuation models, liquefaction potential, site-specific effects, and resonance, all of which are essential for

comprehending the effects of earthquakes in these regions (Aoudia et al., 2000; Bouhadad et al., 2004; Semmane et al., 2005; Laouami et al., 2006; Harbi et al., 2007; Bensalem et al., 2010; Meslem et al., 2010; Laouami and Slimani, 2013; Beneldjouzi et al., 2017; Bourenane et al., 2018; Laouami et al., 2018; Mase et al., 2018; Mase et al., 2020; Tanapalungkorn et al., 2020; Mase and Likitlersuang, 2021; Mase et al., 2021; Qodri et al., 2021; Sukkarak et al., 2021b; Mase et al., 2022a; Mase et al., 2022b).

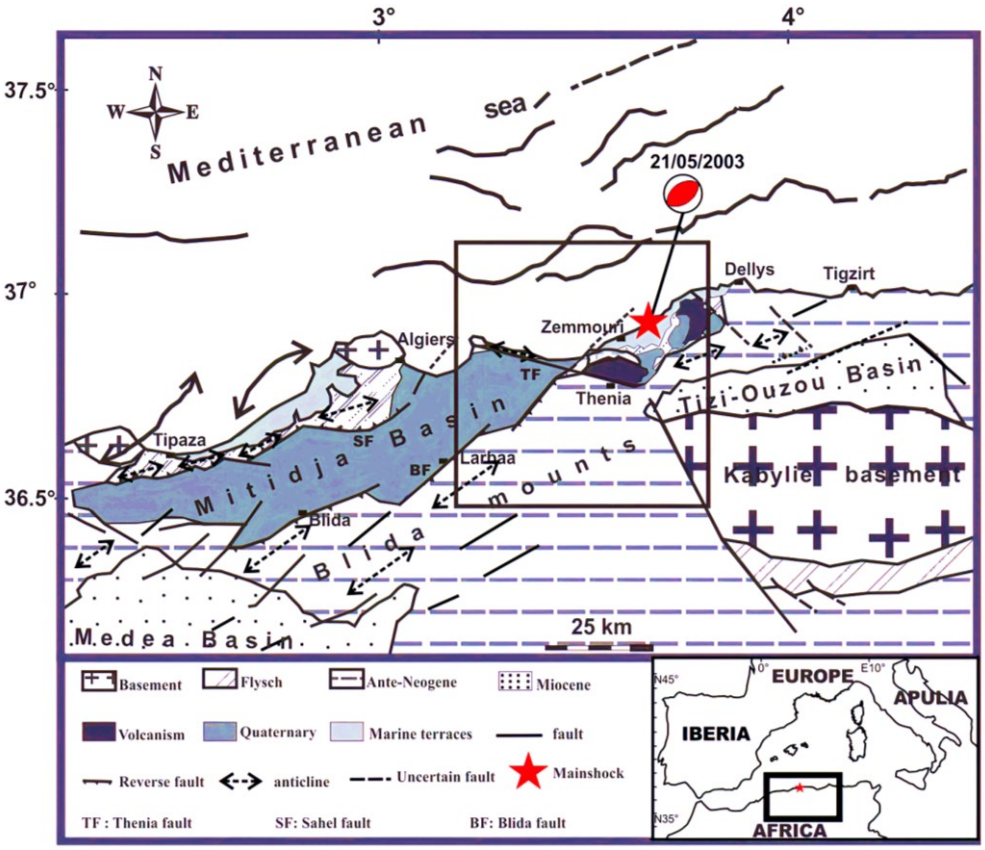

Figure 1 Map of the geological and tectonic framework of the 2003 Boumerdes epicentral area (Kherroubi et al., 2017)

5. CASE STUDY

Section 5, with a total length of 866.60 m in the central part of the metro extension project, was chosen as the study case. The aim is to investigate the behavior of the Algiers metro tunnel under the impact of an earthquake loading (Figure 2). The tunnel is excavated using the shield construction method and a tunnel boring machine (TBM). The tunnel center and water table are 26.5 m and 16.21 m below the ground surface, respectively. The soil is heterogeneous, with four layers. The upper one is made up of 2 m thick embankments. This layer sits on top of a 10 m thick slightly sandy silty clay. The latter rises above a layer of silty-clayey sand and is topped by an 8-meter-thick layer of sandstone. The marl layer below is where the tunnel is excavated; its thickness is 30 meters. Tables 1 and 2 summarize the characteristics of the soil profile and tunnel. The geotechnical soil parameters were carefully and elaborately determined through a combination of laboratory and field tests, following statistical methodology to find characteristic values. Saturated unit weight (γ_{sat}) was developed by saturating the soil samples and determining the weight per unit volume of each unit volume. Dry unit weight (γ_{dry}) was found by drying the soil samples to zero moisture content and determining the weight per unit volume. The Young's modulus in undrained conditions (E_u) was calculated from Pressuremeter Tests (PT) corrected according to Menard's correlation (PTM). The effective cohesion (c') was obtained based on direct shear tests (DST) and the recommendations of Wilun & Starzewski (1972). The undrained cohesion (c_u) was estimated from the Standard Penetration Test (SPT) and PT. The effective friction angle (ϕ') was obtained from correlations with the plasticity index; for non-cohesive soils, SPT and PT were used. Finally, the Poisson's ratio (ν') was estimated using the theoretical relations of Lambe and Whitman, with adjustments to determine the drained (E') and undrained (E_u) deformability moduli. Finally, permeability (k), which is the capacity of the soil to allow the flow of water, it was determined by the laboratory tests of Constant Head (CHT) and Falling Head Permeability Tests (FHPT), in addition to the field tests.

Table 1 Soil characteristics

Properties	Layers			
	Layer 1	Layer 2	Layer 3	Layer 4
Saturated unit weight [kg/m^3]	2000	2100	2100	2000
Dry unit weight [kg/m^3]	1700	1700	1800	1700
Young's modulus [kN/m^2]	10000	37000	73000	76000
Poisson's coefficient [/]	0.3	0.3	0.3	0.3
Cohesion [kN/m^2]	-	31	10	53
Friction angle [°]	20	21	35	20
Permeability [m/s]	-	10^{-8}	10^{-4}	10^{-8}

Table 2 Tunnel characteristics

EA	*EI*	*γ*	*υ*	D_{out}	D_{in}
[kN/m]	[kN m^2/m]	[KN/m^2]	-	[m]	[m]
1.575×10^7	2.658×10^5	25	0.20	10.20	09.30

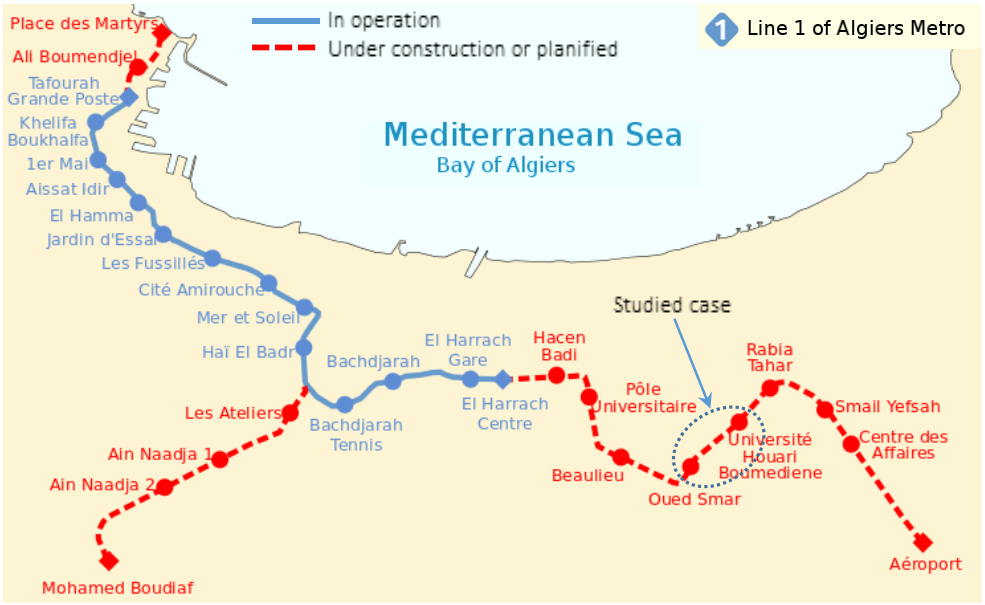

Figure 2 Algiers metro lines: studied case position (Wikipedia, 2023)

6. RESULTS AND DISCUSSIONS

The internal forces in the tunnel of the Algiers metro extension project were studied using FE seismic analysis compared to analytical solutions. Figures 4 and 5 show the horizontal and vertical accelerogram components of the earthquake, recorded at Algiers' Dar El Beida seismic station, which is 29 km away from the epicenter (Laouami et al., 2006). Damping coefficients, α and β, for RC liners and the surrounding soil, were determined using free vibration analysis. The fundamental and third frequencies of the site were determined using the DEEPSOIL software©, resulting in SF = 1.70 Hz and 5SF = 8.50 Hz, respectively. Equation (2) calculated the α and β after knowing the SF and 5SF. Given a 10% damping of the surrounding soil, α and β were calculated as 0.308 and 0.0045. For 2% damping in RC liners, the values $\alpha = 0.123$ and $\beta = 0.0018$ were used. The boundary dimensions of the studied model were chosen based on sensitivity analysis up to a stable analysis (Figure 3). Fixed boundary conditions were applied at the bottom and lateral boundaries.

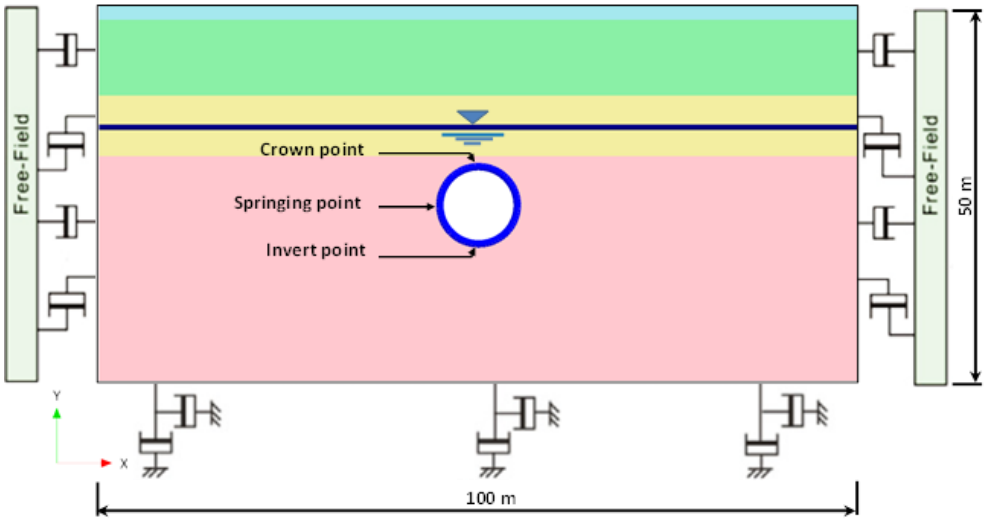

Figure 3 2D Numerical model built with Plaxis

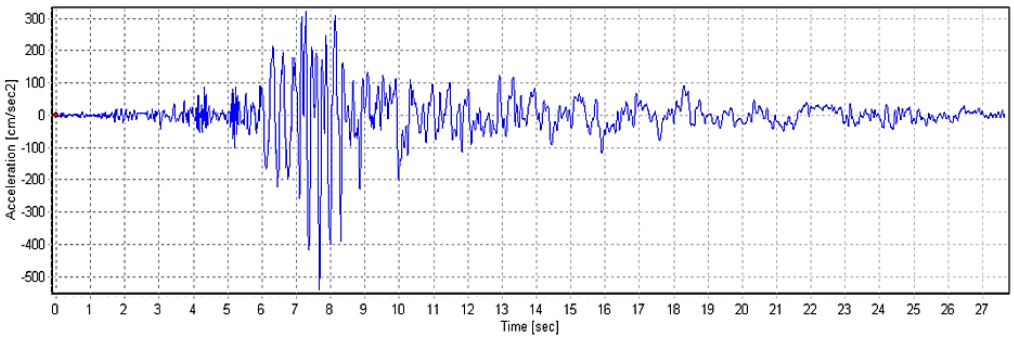

Figure 4 Horizontal accelerogram component of the 2003 Boumerdes earthquake

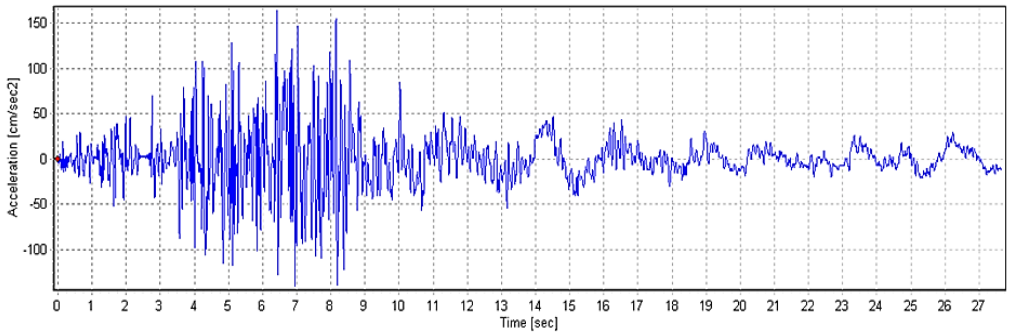

Figure 5 Vertical accelerogram component of the 2003 Boumerdes earthquake

The shear strain value γ_{max} is an important parameter in the internal forces calculations in the analytical solutions discussed above. Figure 6 depicts the results of an equivalent linear site response analysis using DEEPSOIL program to plot the cumulative displacement profile. The slope of the cumulative displacement profile within the tunnel horizon, from a depth of 21.4 m to 31.6 m, can be used to calculate the shear strain within the tunnel horizon. In this study, the shear and vertical strains values were determined to be γ_{max} = 0.26 and $\varepsilon_{max} = 0.16$. The ε_{max} value can be deduced from γ_{max} and V_{max} values using Equations 26 and 29. Figure 7 compares the results of the FE analysis (FEA) with analytical solutions for the horizontal seismic component, considering varying contraction coefficient values (volume loss ratio, VL). This figure demonstrates that varying the VL value influences the behavior of internal forces. Specifically, the axial force in the tunnel liner takes negative values when VL < 1%, alternates between positive and negative values when 1% ≤ VL ≤ 1.50%, and becomes consistently positive for VL > 1.50%. This variation tendency can also be observed in some works, such as (Chehade and Shahrour, 2008; Amorosi and Boldini, 2009; Argyroudis and Pitilakis, 2012; Kontoe et al., 2014). Convergence between the solutions by Wang, Bobet (2010), Park et al., and the FE results are observed at VL = 1.25%. The values obtained from Bobet (2003) and Penzien's solutions are located between the results for two FE cases with VL values of 0.75% and 1.75%. Penzien's solution values for shear force practically align with the envelope of the FE values. A similar tendency is observed for the bending moment, where analytical solutions are generally within the envelope of the FE values, except for Bobet's (2003) solution, which shows larger values. As depicted in Figure 9, the internal forces exhibit the same behavior under the impact of the vertical component as observed in the horizontal component. In Figures 8 and 10, the distribution of internal forces in the tunnel liner is plotted using Plaxis software, with VL = 1.25% for the horizontal component and VL = 1.5% for the vertical component, respectively.

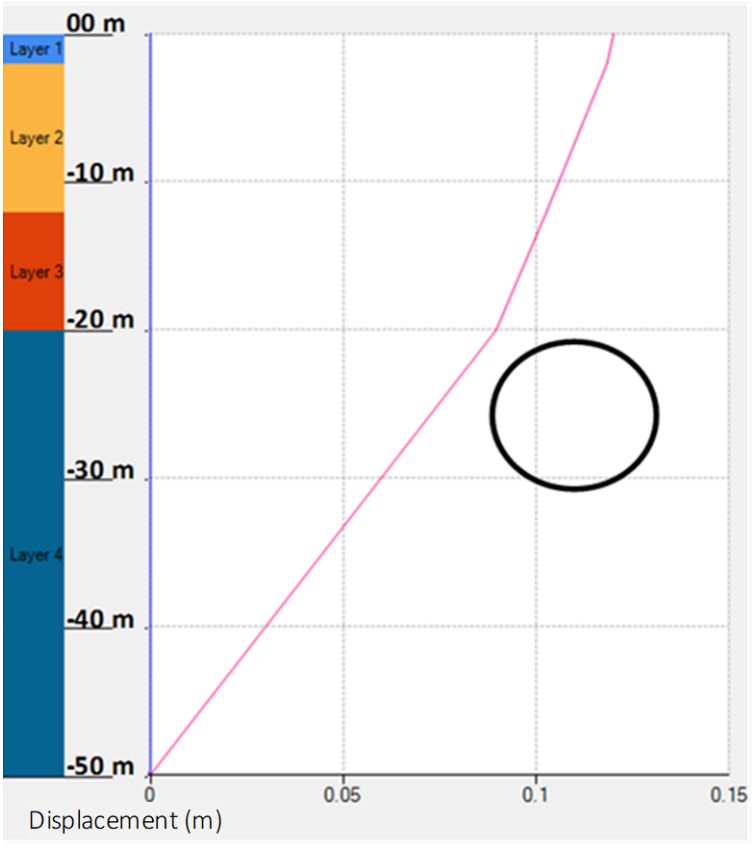

Figure 6 Cumulative displacement of the soil profile performed with DEEPSOIL

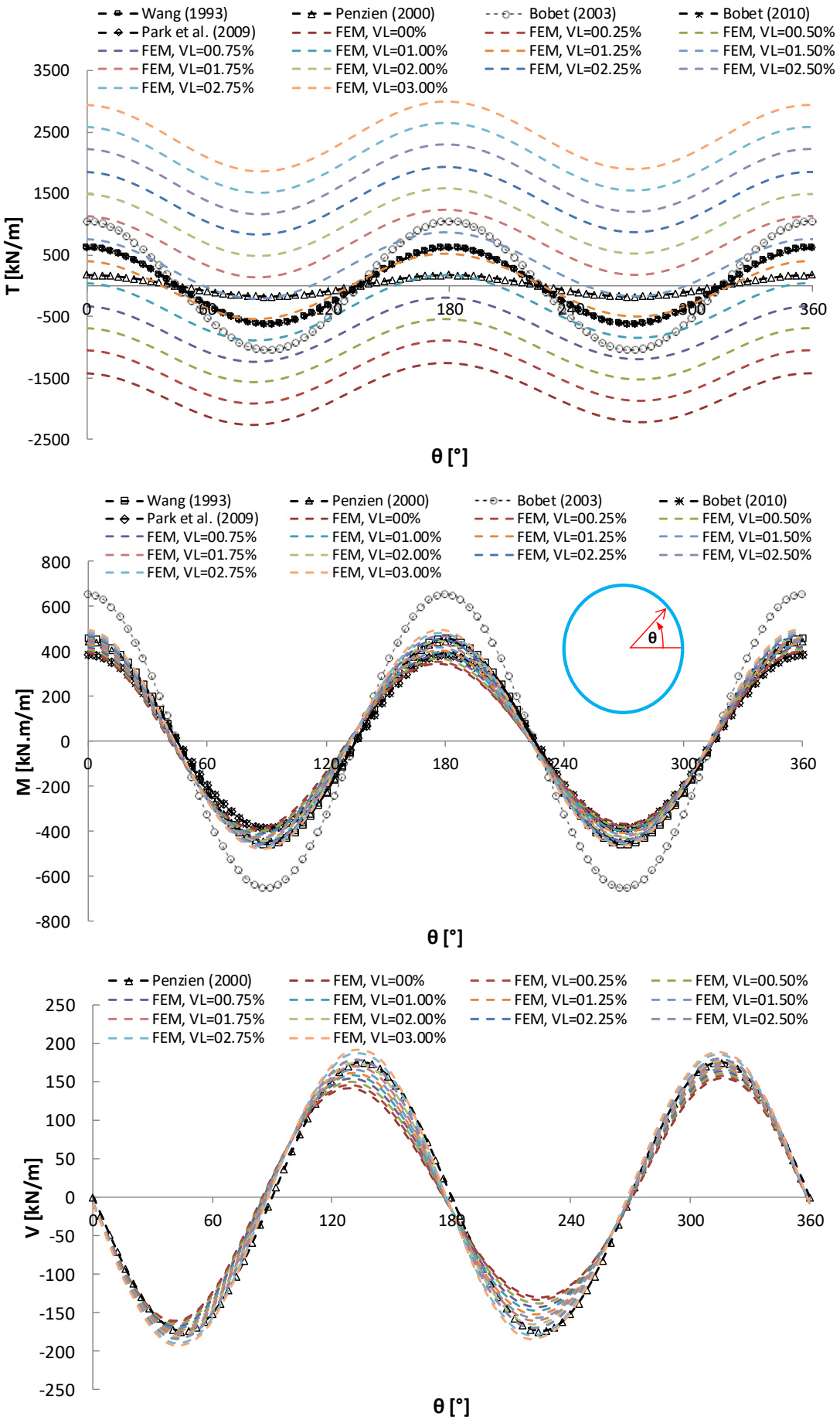

Figure 7 Internal forces distribution in the tunnel liner due to horizontal seismic component; comparison between analytical solutions and FEA

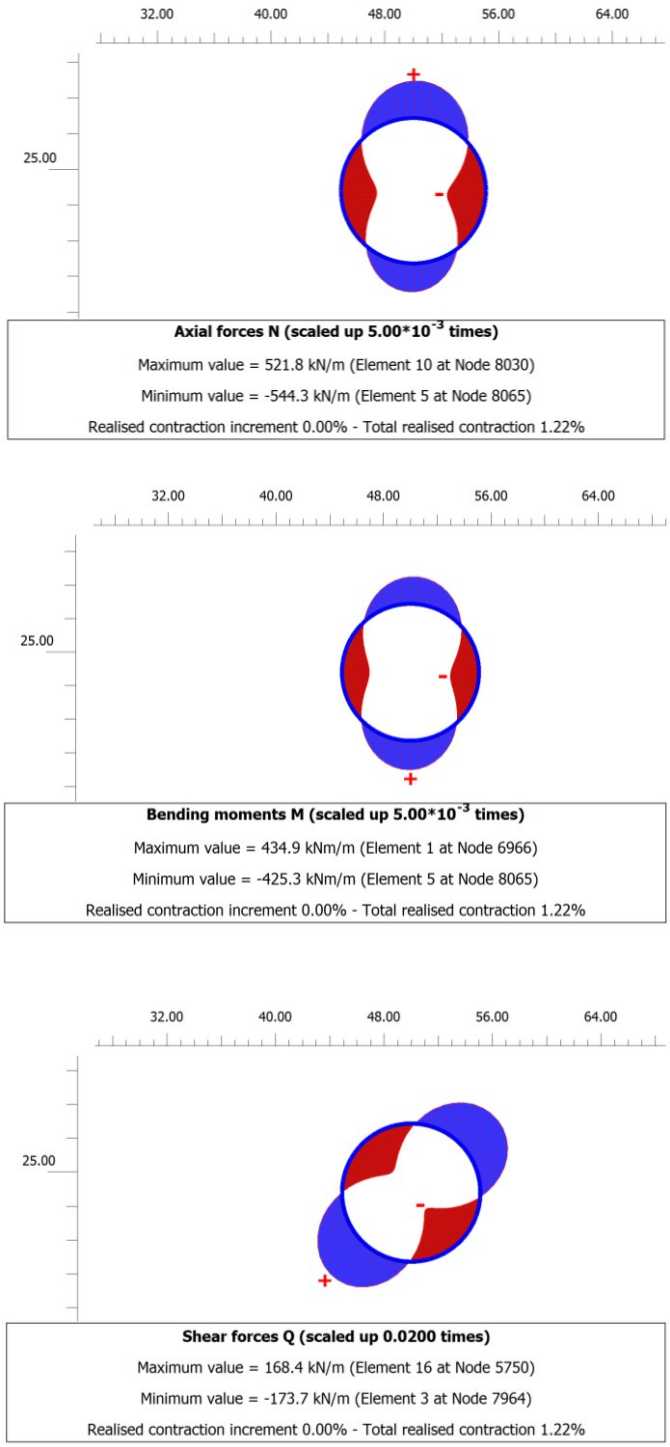

Figure 8 Internal forces distribution in the tunnel liner due to horizontal seismic component; plotted by Plaxis for VL = 1.25%

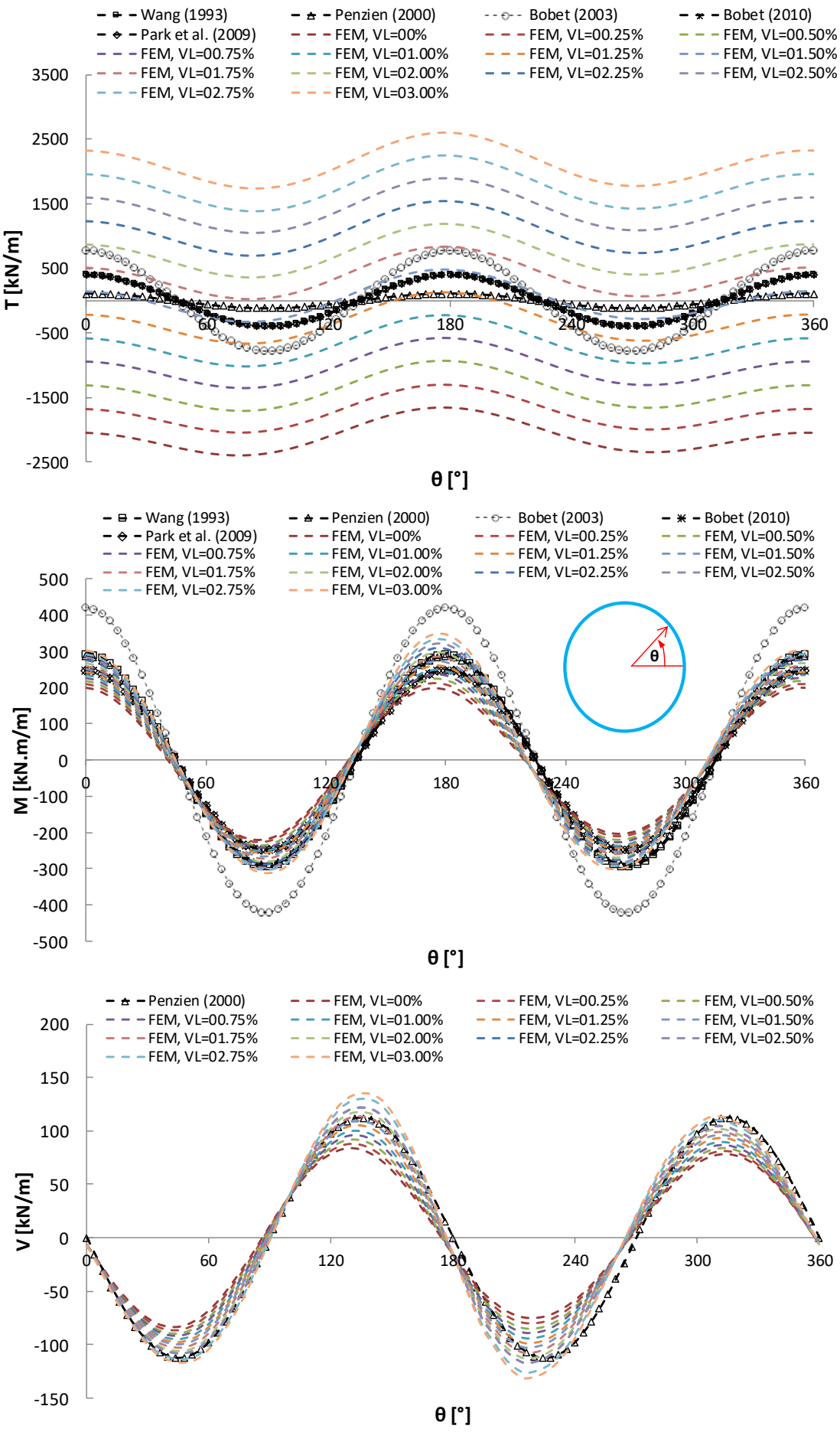

Figure 9 Internal forces distribution in the tunnel liner; comparison between analytical solutions and FEA

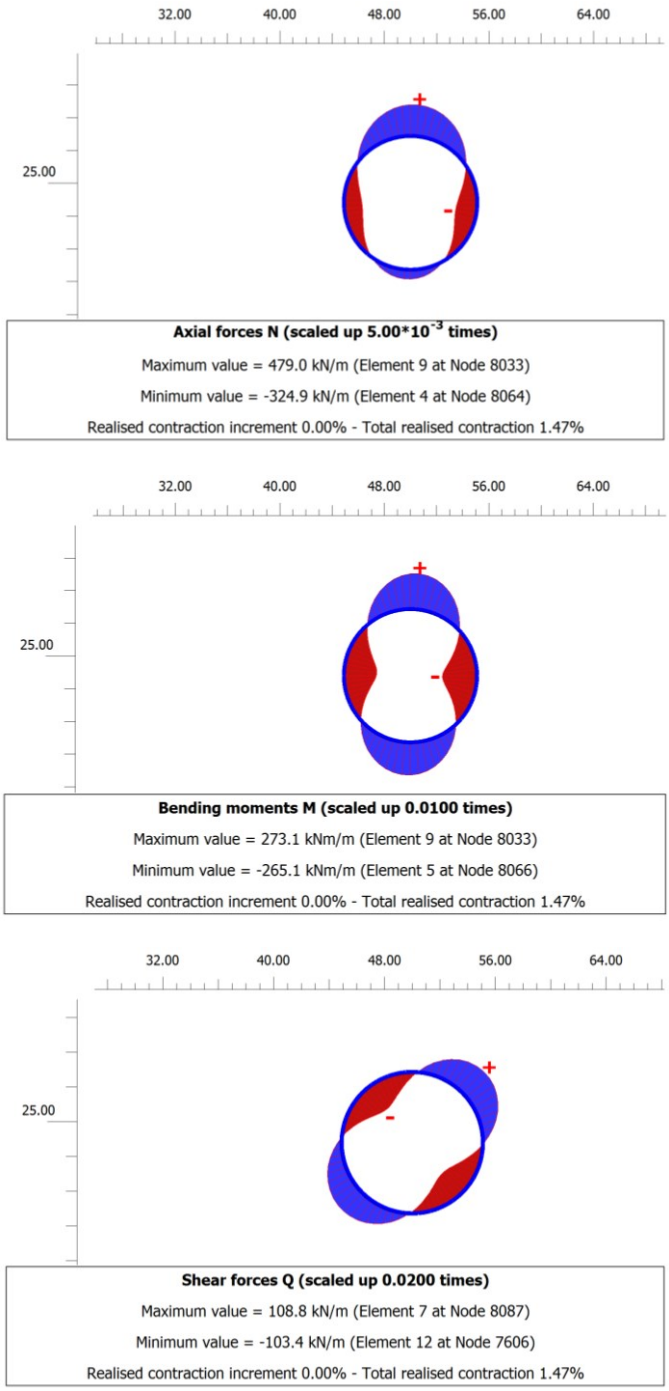

Figure 10 Internal forces distribution in the tunnel liner due to vertical seismic component; plotted by Plaxis for VL = 1.5%

By varying the contraction coefficient values, Figure 11 compares the absolute internal forces of the analytical solutions with FEA results due to horizontal seismic component. The absolute axial thrust decreases as the contraction coefficient value increases until it enters the envelope of the analytical solutions values, then increases again at VL = 1.25%. The shear force values of the FE elastic analysis coincide with Penzien's solution results of 1% ≤ VL ≤2% and the difference can reach up to ±8% outside of this interval. Increasing the contraction coefficient increases the FE bending moment values while remaining within the analytical solution envelope values. These values coincide with the solutions proposed by Bobet (2010) and Park et al. when VL ≤ 0.75%. Moreover, the values agree with Wang and Penzien's solutions when VL ≥ 1.75%. The variation range can be up to 23%.

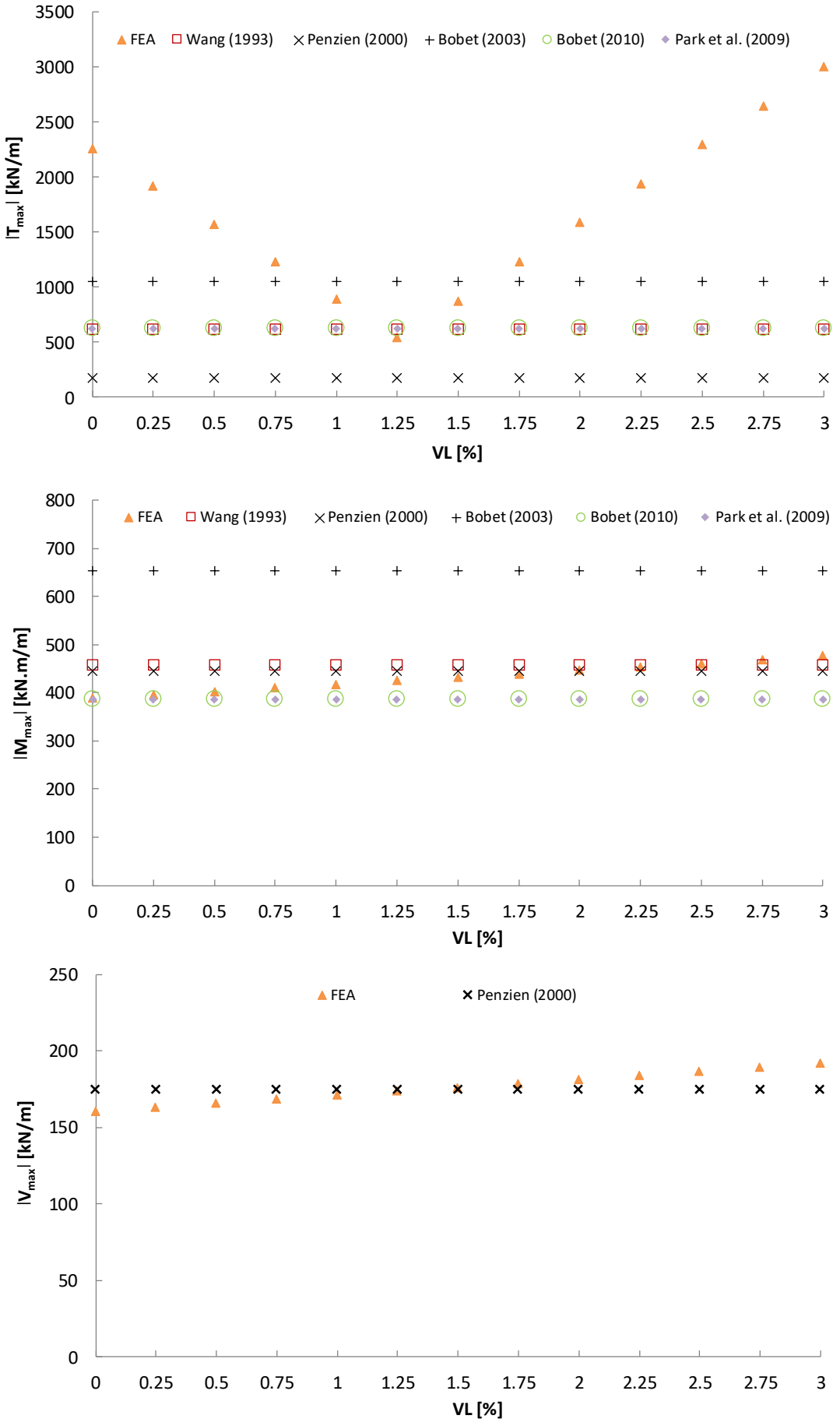

Figure 11 Absolute internal forces in the tunnel liner due to horizontal seismic component; comparison between analytical solutions and FEA

Figure 12 illustrates the comparison between the absolute internal forces of analytical solutions and the results from FEA for the vertical seismic component. The absolute axial thrust initially decreases with an increase in the contraction coefficient value until it falls within the envelope of analytical solutions, then rises again at VL = 1.5%. The shear force values from the FE analysis align with Penzien's solution results for 1.25% ≤ VL ≤ 2.25%, with differences reaching up to ±23% outside this range. The increase in the contraction coefficient raises the FE bending moment values, remaining predominantly within the analytical solution range. These values approach the solutions suggested by Bobet (2010) and Park et al. when VL ≤ 1.5% and those of Wang and Penzien when VL ≥ 1.5%. The range of variation can extend up to ±10%.

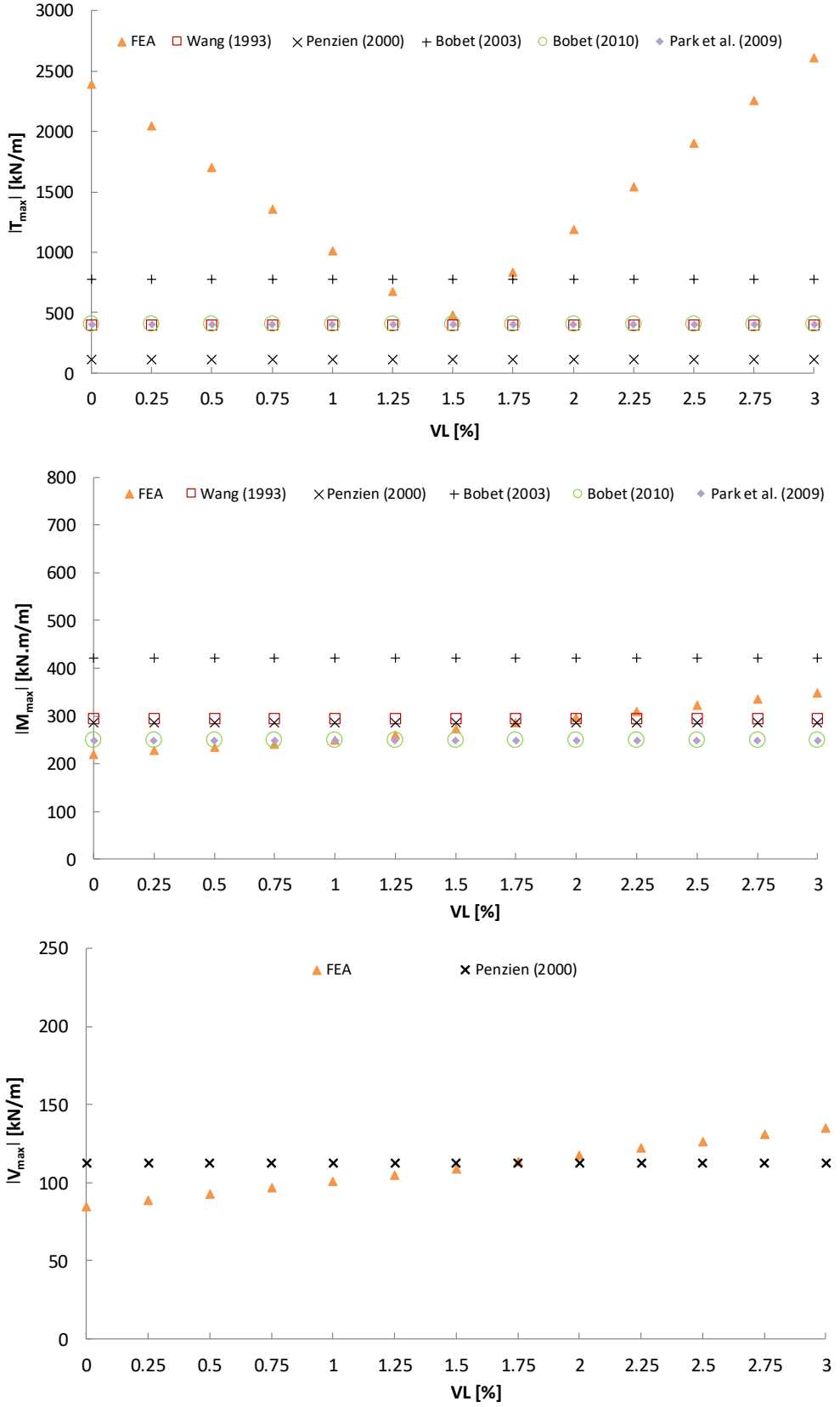

Figure 12 Absolute internal forces in the tunnel liner due to vertical seismic component; comparison between analytical solutions and FEA

Figures 13 and 14 illustrate the total principal stresses resulting from the horizontal and vertical seismic components, taking into account the effect of the VL ratio. Increasing the VL ratio value from 0% to 3% can lead to a 62% increase in total principal stresses around the tunnel under the impact of the horizontal seismic component and a 50% increase for the vertical component. This is evident in the degree of stress concentration around the tunnel.

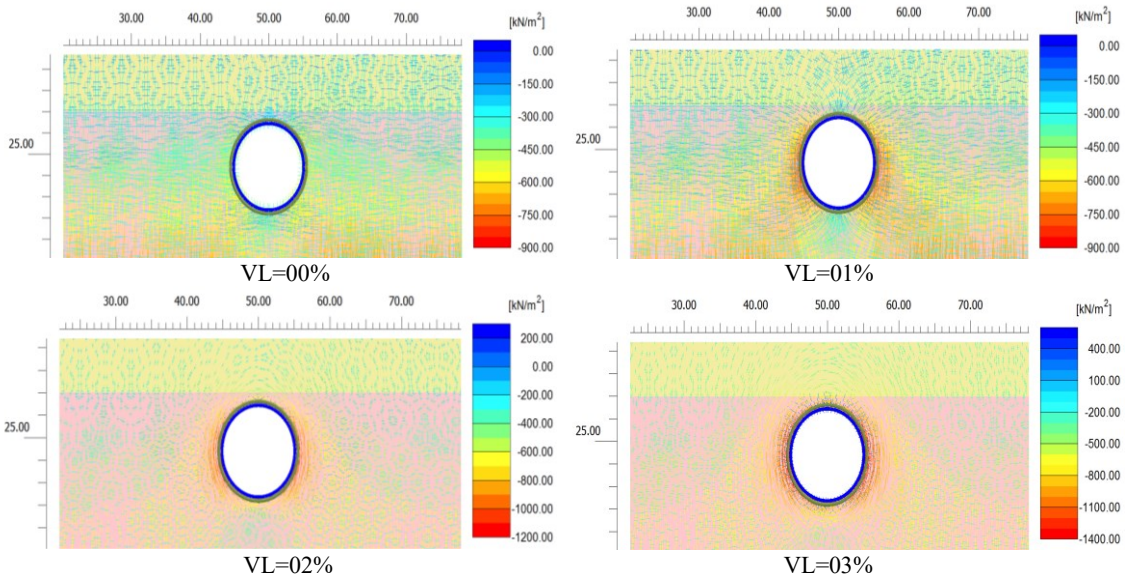

Figure 13 Total principal stresses due to horizontal seismic component

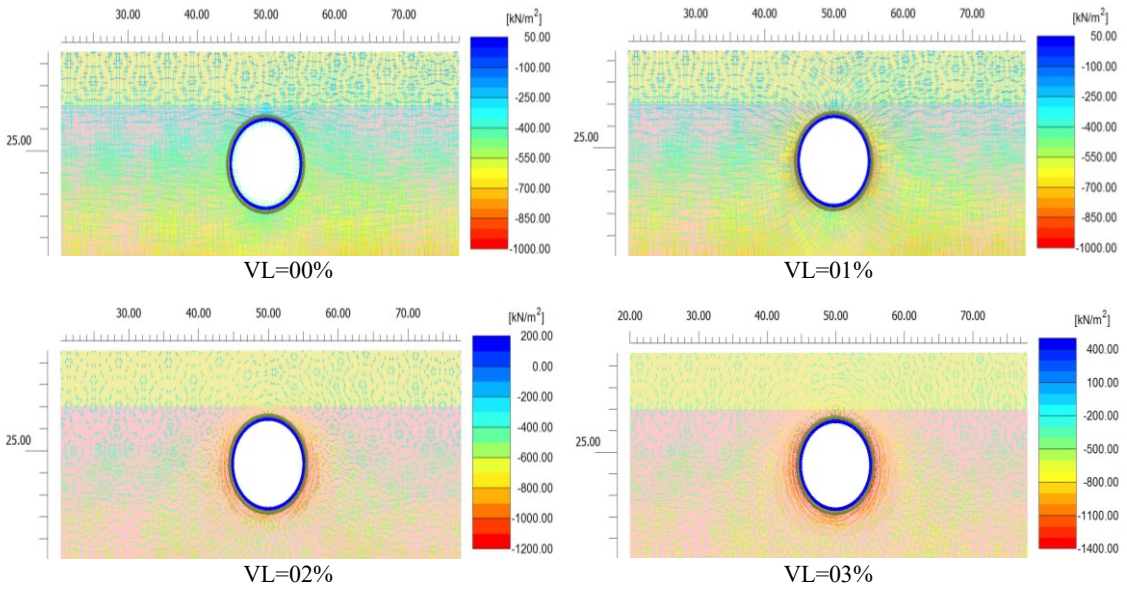

Figure 14 Total principal stresses due to vertical seismic component

7. CONCLUSIONS

This paper studies the complex relationship between the contraction coefficient and internal forces in circular tunnels under seismic loading. Through FEM analysis and comparison with simplified analytical approaches, it is demonstrated that variation in the contraction coefficient significantly impacts axial thrust, shear force, bending moment, and total principal stresses. On the other hand, excellent alignment with simplified methods for the specific contraction coefficient ranges offers practical utility, in particular during preliminary design stages. These are quite notable results considering this study, yet its scope is limited to investigations relating to elastic forces and to contractive coefficients, and seismic loading. However, the study results are valuable for tunnel engineering, guiding design modifications, and safety evaluations. Future research should explore nonlinear behaviors, validate the results using field data, and enhance seismic design practices for underground structures.

8. REFERENCES

Achouri, A., and Amrane, M. N. (2020). "Effect of Structures Density and Tunnel Depth on the Tunnel-Soil-Structures Dynamical Interaction." *Pollack Periodica*, 15(1), 91-102. https://doi.org/10.1556/606.2020.15.1.9.

Achouri, A., and Amrane, M. N. (2021). "Effects of the Superficial Layer Overlying a Half-Space on the Tunnel-Soil-RC Building Dynamical Interaction." *International Journal of Structural Engineering*, 11(3), 270-293. https://doi.org/10.1504/IJSTRUCTE.2021.116522.

Alielahi, H., and Feizi, D. (2021). "Numerical Study on Dynamic Effects of Soil-Tunnel-Structure Interaction." *International Journal of Civil Engineering*, 19(11), 1339-1355. https://doi.org/10.1007/s40999-021-00642-8.

Amorosi, A., and Boldini, D. (2009). "Numerical Modelling of the Transverse Dynamic Behaviour of Circular Tunnels in Clayey Soils." *Soil Dynamics and Earthquake Engineering*, 29(6), 1059-1072. https://doi.org/10.1016/j.soildyn.2008.12.004.

Aoudia, A., Vaccari, F., Suhadolc, P., and Meghraoui, M. (2000). "Seismogenic Potential and Earthquake Hazard Assessment in the Tell Atlas of Algeria." *Journal of Seismology*, 4, 79-98. https://doi.org/10.1023/A:1009848714019.

Argyroudis, S., and Pitilakis, K. (2012). "Seismic Fragility Curves of Shallow Tunnels in Alluvial Deposits." *Soil Dynamics and Earthquake Engineering*, 35, 1-12. https://doi.org/10.1016/j.soildyn.2011.11.004.

Asheghabadi, M. S., and Matinmanesh, H. (2011). "Finite Element Seismic Analysis of Cylindrical Tunnel in Sandy Soils with Consideration of Soil-Tunnel Interaction." *Procedia Engineering*, 14, 3162-3169. https://doi.org/10.1016/j.proeng.2011.07.399.

Beneldjouzi, M., Laouami, N., and Slimani, A. (2017). "Numerical and Random Simulation Procedure for Preliminary Local Site Characterization and Site Factor Assessing." *Earthquake and Structures*, 13(1), 79-87. https://doi.org/10.12989/eas.2017.13.1.079.

Bensalem, R., Chatelain, J.-L., Machane, D., Oubaiche, E. H., Hellel, M., Guillier, B., Djeddi, M., and Djadia, L. (2010). "Ambient Vibration Techniques Applied to Explain Heavy Damages Caused in Corso (Algeria) by the 2003 Boumerdes Earthquake: Understanding Seismic Amplification due to Gentle Slopes." *Seismological Research Letters*, 81(6), 928-940. https://doi.org/10.1785/gssrl.81.6.928.

Bilotta, E., Lanzano, G., Russo, G., Silvestri, F., and Madabhushi, G. (2009). *Proceedings of the 17th International Conference on Soil Mechanics and Geotechnical Engineering (Volumes 1, 2, 3 and 4). Alexandria, Egypt. IOS Press.*

Bobet, A. (2003) "Effect of Pore Water Pressure on Tunnel Support during Static and Seismic Loading." *Tunnelling and Underground Space Technology*, 18(4), 377-393. https://doi.org/10.1016/S0886-7798(03)00008-7.

Bobet, A. (2010). "Drained and Undrained Response of Deep Tunnels Subjected to Far-Field Shear Loading." *Tunnelling and Underground Space Technology*, 25(1), 1-31. https://doi.org/10.1016/j.tust.2009.08.001.

Bouhadad, Y., Nour, A., Slimani, A., Laouami, N., and Belhai, D. (2004). "The Boumerdès (Algeria) Earthquake of May 21, 2003 (M W= 6.8): Ground Deformation and Intensity." *Journal of Seismology*, 8, 497-506. https://doi.org/10.1007/s10950-004-4838-0.

Bourenane, H., Bouhadad, Y., and Tas, M. (2018). "Liquefaction Hazard Mapping in the City of Boumerdès, Northern Algeria." *Bulletin of Engineering Geology and the Environment*, 77, 1473-1489. https://doi.org/10.1007/s10064-017-1137-x.

Brinkgreve, R. B. J. (2003). "PLAXIS 2D Scientific Manual." 8 edn. Tokyo: *Balkema*.

Chehade, F. H., and Shahrour, I. (2008). "Numerical Analysis of the Interaction between Twin-Tunnels: Influence of the Relative Position and Construction Procedure." *Tunnelling and Underground Space Technology*, 23(2), 210-214. https://doi.org/10.1016/j.tust.2007.03.004.

Chen, J., Shi, X., and Li, J. (2010). "Shaking Table Test of Utility Tunnel under Non-Uniform Earthquake Wave Excitation." *Soil Dynamics and Earthquake Engineering*, 30(11), 1400-1416. https://doi.org/10.1016/j.soildyn.2010.06.014.

Cheng, R., Chen, W., Hao, H., and Li, J. (2021). "A State-of-the-Art Review of Road Tunnel Subjected to Blast Loads." *Tunnelling Underground Space Technology*, 112, 103911. https://doi.org/10.1016/j.tust.2021.103911.

Choudhury, D., Patil, M., Ranjith, P., and Zhao, J. (2019). "Dynamic Tunnel–Soil Interaction in Soft Soils Considering Site-Specific Seismic Ground Response." *Frontiers in Geotechnical Engineering*, 249-271. https://doi.org/10.1007/978-981-13-5871-5_12.

Corigliano, M. (2007). "Seismic Response of Deep Tunnels in Near-Fault Conditions." *Politecnico di Torino*.

Corigliano, M., Scandella, L., Lai, C. G., and Paolucci, R. (2011). "Seismic Analysis of Deep Tunnels in near Fault Conditions: A Case Study in Southern Italy." *Bulletin of Earthquake Engineering*, 9, 975-995. https://doi.org/10.1007/s10518-011-9249-3.

Govindasamy, D., Ismail, M. A. M., Zaki, M. F. M., Ken, T. Y., Cheah, F., and Likitlersuang, S. (2020). "Assessment of the Twin-Tunnel Interaction Mechanism in Kenny Hill Formation Using Contraction Ratio Method." *Indian Geotechnical Journal*, 50, 825-837. https://doi.org/10.1007/s40098-020-00411-9.

Harbi, A., Maouche, S., Vaccari, F., Aoudia, A., Oussadou, F., Panza, G., and Benouar, D. (2007). "Seismicity, Seismic Input and Site Effects in the Sahel—Algiers Region (North Algeria)." *Soil Dynamics and Earthquake Engineering*, 27(5), 427-447. https://doi.org/10.1016/j.soildyn.2006.10.002.

Hashash, Y. M., Park, D., John, I., and Yao, C. (2005). "Ovaling Deformations of Circular Tunnels under Seismic Loading, An Update on Seismic Design and Analysis of Underground Structures." *Tunnelling Underground Space Technology*, 20(5), 435-441. https://doi.org/10.1016/j.tust.2005.02.004.

Hilber, H. M., Hughes, T. J., and Taylor, R. L. (1977). "Improved Numerical Dissipation for Time Integration Algorithms in Structural Dynamics." *Earthquake Engineering and Structural Dynamics*, 5(3), 283-292. https://doi.org/10.1002/eqe.4290050306.

Höeg, K. (1968). "Stresses against Underground Structural Cylinders." *Journal of the Soil Mechanics Foundations Division*, 94(4), 833-858. https://doi.org/10.1061/JSFEAQ.0001175.

Kherroubi, A., Yelles-Chaouche, A., Koulakov, I., Déverchère, J., Beldjoudi, H., Haned, A., Semmane, F., and Aidi, C. (2017). "Full Aftershock Sequence of the Mw 6.9 2003 Boumerdes Earthquake, Algeria: Space–time Distribution, Local Tomography and Seismotectonic Implications." *Pure and Applied Geophysics*, 174, 2495-2521. https://doi.org/10.1007/s00024-017-1571-5.

Kontoe, S., Avgerinos, V., and Potts, D. (2014). "Numerical Validation of Analytical Solutions and their Use for Equivalent-Linear Seismic Analysis of Circular Tunnels." *Soil Dynamics and Earthquake Engineering*, 66, 206-219. https://doi.org/10.1016/j.soildyn.2014.07.004.

Kuhlemeyer, R. L., and Lysmer, J. (1973). "Finite Element Method Accuracy for Wave Propagation Problems." *Soil Mechanics and Foundation Division*, 99(5), 421-427. https://doi.org/10.1061/JSFEAQ.0001885.

Kwok, A. O., Stewart, J. P., Hashash, Y. M., Matasovic, N., Pyke, R., Wang, Z., and Yang, Z. (2007). "Use of Exact Solutions of Wave Propagation Problems to Guide Implementation of Nonlinear Seismic Ground Response Analysis Procedures." *Journal of Geotechnical and Geoenvironmental Engineering*, 133(11), 1385-1398. https://doi.org/10.1061/(ASCE)1090-0241(2007)133:11(1385).

Lanzano, G., Bilotta, E., Russo, G., and Silvestri, F. (2015). "Experimental and Numerical Study on Circular Tunnels under Seismic Loading." *European Journal of Environmental Civil Engineering*, 19(5), 539-563. https://doi.org/10.1080/19648189.2014.893211.

Laouami, N., and Slimani, A. (2013). "Earthquake Induced Site Effect in the Algiers–Boumerdes Region: Relation Between Spectral Ratios Higher Peaks and Observed Damage During the May 21st Mw 6.8 Boumerdes Earthquake (Algeria)." *Pure and Applied Geophysics*, 170, 1785-1801. https://doi.org/10.1007/s00024-012-0612-3.

Laouami, N., Slimani, A., Bouhadad, Y., Chatelain, J.-L., and Nour, A. (2006). "Evidence for Fault-Related Directionality and Localized Site Effects from Strong Motion Recordings of the 2003 Boumerdes (Algeria) Earthquake: Consequences on Damage Distribution and the Algerian Seismic Code." *Soil Dynamics and Earthquake Engineering*, 26(11), 991-1003. https://doi.org/10.1016/j.soildyn.2006.03.006.

Laouami, N., Slimani, A., and Larbes, S. (2018). "Ground Motion Prediction Equations for Algeria and Surrounding Region using Site Classification Based H/V Spectral Ratio." *Bulletin of Earthquake Engineering*, 16, 2653-2684. https://doi.org/10.1007/s10518-018-0310-3.

Likitlersuang, S., Chheng, C., Surarak, C., and Balasubramaniam, A. (2018). "Strength and Stiffness Parameters of Bangkok Clays for

Finite Element Analysis." *Geotechnical Engineering*, 49(2), 150-156. https://10.14456/seagj.2018.46.

Likitlersuang, S., Surarak, C., Suwansawat, S., Wanatowski, D., Oh, E., and Balasubramaniam, A. (2014). "Simplified Finite-Element Modelling for Tunnelling-Induced Settlements." *Geotechnical Research*, 1(4), 133-152. https://doi.org/10.1680/gr.14.00016.

Likitlersuang, S., Surarak, C., Wanatowski, D., Oh, E., and Balasubramaniam, A. (2013a). "Geotechnical Parameters from Pressuremeter Tests for MRT Blue Line Extension in Bangkok." *Geomechanics and Engineering: An International Journal*, 5(2), 99-118. https://10.12989/gae.2013.5.2.099.

Likitlersuang, S., Teachavorasinskun, S., Surarak, C., Oh, E., and Balasubramaniam, A. (2013b). "Small Strain Stiffness and Stiffness Degradation Curve of Bangkok Clays." *Soils and Foundations*, 53(4), 498-509. https://doi.org/10.1016/j.sandf.2013.06.003.

Lysmer, J., and Kuhlemeyer, R. L. (1969). "Finite Dynamic Model for Infinite Media." *Journal of the Engineering Mechanics Division*, 95(4), 859-878. https://doi.org/10.1061/JMCEA3.0001144.

Mahsas, A., Lammali, K., Yelles, K., Calais, E., Freed, A., and Briole, P. (2008). "Shallow Afterslip Following the 2003 May 21, Mw = 6.9 Boumerdes Earthquake, Algeria." *Geophysical Journal International*, 172(1), 155-166. https://doi.org/10.1111/j.1365-246X.2007.03594.x.

Mase, L. Z., and Likitlersuang, S. (2021). "Implementation of Seismic Ground Response Analysis in Estimating Liquefaction Potential in Northern Thailand." *Indonesian Journal on Geoscience*, 8(3). https://10.17014/ijog.8.3.371-383.

Mase, L. Z., Likitlersuang, S., and Tobita, T. (2018). "Analysis of Seismic Ground Response Caused during Strong Earthquake in Northern Thailand." *Soil Dynamics and Earthquake Engineering*, 114, 113-126. https://doi.org/10.1016/j.soildyn.2018.07.006.

Mase, L. Z., Likitlersuang, S., and Tobita, T. (2021). "Ground Motion Parameters and Resonance Effect during Strong Earthquake in Northern Thailand." *Geotechnical and Geological Engineering*, 39(3), 2207-2219. https://doi.org/10.1007/s10706-020-01619-5.

Mase, L. Z., Likitlersuang, S., and Tobita, T. (2022a). "Verification of Liquefaction Potential during the Strong Earthquake at the Border of Thailand-Myanmar." *Journal of Earthquake Engineering*, 26(4), 2023-2050. https://doi.org/10.1080/13632469.2020.17513 46.

Mase, L. Z., Likitlersuang, S., Tobita, T., Chaiprakaikeow, S., and Soralump, S. (2020). "Local Site Investigation of Liquefied Soils Caused by Earthquake in Northern Thailand." *Journal of Earthquake Engineering*, 24(7), 1181-1204. https://doi.org/10.1080/13632469.2018.1469441.

Mase, L. Z., Tanapalungkorn, W., Likitlersuang, S., Ueda, K., and Tobita, T. (2022b). "Liquefaction Analysis of Izumio Sands under Variation of Ground Motions during Strong Earthquake in Osaka, Japan." *Soils and Foundations*, 62(5), 101218. https://doi.org/10.1016/j.sandf.2022.101218.

Meslem, A., Yamazaki, F., Maruyama, Y., Benouar, D., Laouami, N., and Benkaci, N. (2010). "Site-Response Characteristics Evaluated from Strong Motion Records of the 2003 Boumerdes, Algeria, Earthquake." *Earthquake Spectra*, 26(3), 803-823. https://doi.org/10.1193/1.3459158.

Muenpetch, N., Keawsawasvong, S., Komolvilas, V., and Likitlersuang, S. (2023). "Numerical Investigation on Impact of Excavations in Influence Zone of Existing MRT Tunnels." *Geomechanics and Geoengineering*, 1-20. https://doi.org/10.1080/17486025.2023.2226107.

Park, K.-H., Tantayopin, K., Tontavanich, B., and Owatsiriwong, A. (2009). "Analytical Solution for Seismic-Induced Ovaling of Circular Tunnel Lining under No-Slip Interface Conditions: A Revisit." *Tunnelling Underground Space Technology*, 24(2), 231-235. https://doi.org/10.1016/j.tust.2008.07.001.

Peck, R. B., Hendron, A., and Mohraz, B. (1972). *Rapid Excavation and Tunnelling Conference. Chicago, IL.*

Penzien, J. (2000). "Seismically Induced Racking of Tunnel Linings." *Earthquake Engineering Structural Dynamics*, 29(5), 683-691. https://doi.org/10.1002/(SICI)1096-9845(200005)29:5<683::AID-EQE932>3.0.CO;2-1.

Penzien, J., and Wu, C. L. (1998). "Stresses in Linings of Bored Tunnels." *Earthquake Engineering Structural Dynamics*, 27(3), 283-300. https://doi.org/10.1002/(SICI)1096-9845(199803)27:3<283::AID-EQE732>3.0.CO;2-T.

Phutthananon, C., Lertkultanon, S., Jongpradist, P., Duangsano, O., Likitlersuang, S., and Jamsawang, P. (2023). "Numerical Investigation on the Responses of Existing Single Piles due to Adjacent Twin Tunneling Considering the Lagging Distance." *Underground Space*, 11, 171-188. https://doi.org/10.1016/j.undsp.2022.12.005.

Qodri, M. F., Mase, L. Z., and Likitlersuang, S. (2021). "Non-Linear Site Response Analysis of Bangkok Subsoils due to Earthquakes Triggered by Three Pagodas Fault." *Engineering Journal*, 25(1), 43-52. https://doi.org/10.4186/ej.2021.25.1.43.

Salemi, A., Mikaeil, R., and Haghshenas, S. S. (2018). "Integration of Finite Difference Method and Genetic Algorithm to Seismic Analysis of Circular Shallow Tunnels (Case study: Tabriz Urban Railway Tunnels)." *KSCE Journal of Civil Engineering*, 22, 1978-1990. https://doi.org/10.1007/s12205-017-2039-y.

Sandoval, E., and Bobet, A. (2017). "Effect of Frequency and Rlexibility Ratio on the Seismic Response of Deep Tunnels." 2(2), 125-133. https://doi.org/10.1016/j.soildyn.2020.106421.

Sandoval, E., and Bobet, A. (2020). "Effect of Input Frequency on the Seismic Response of Deep Circular Tunnels." *Soil Dynamics and Earthquake Engineering*, 139, 106421. https://doi.org/10.1016/j.soildyn.2020.106421.

Semmane, F., Campillo, M., and Cotton, F. (2005). "Fault Location and Source Process of the Boumerdes, Algeria, Earthquake Inferred from Geodetic and Strong Motion Data." *Geophysical Research Letters*, 32(1). https://doi.org/10.1029/2004GL021268.

Singh, M., Viladkar, M. N., and Samadhiya, N. K. (2017). "Seismic Analysis of Delhi Metro Underground Tunnels." *Indian Geotechnical Journal*, 47, 67-83. https://doi.org/10.1007/s40098-016-0203-9.

Sukkarak, R., Likitlersuang, S., Jongpradist, P., and Jamsawang, P. (2021a). "Strength and Stiffness Parameters for Hardening Soil Model of Rockfill Materials." *Soils and Foundations*, 61(6), 1597-1614. https://doi.org/10.1016/j.sandf.2021.09.007.

Sukkarak, R., Tanapalungkorn, W., Likitlersuang, S., and Ueda, K. (2021b). "Liquefaction Analysis of Sandy Soil during Strong Earthquake in Northern Thailand." *Soils and Foundations*, 61(5), 1302-1318. https://doi.org/10.1016/j.sandf.2021.07.003.

Sun, Q., Dias, D., and e Sousa, L. R. (2020). "Soft Soil Layer-Tunnel Interaction under Seismic Loading." *Tunnelling and Underground Space Technology*, 98, 103-329. https://doi.org/10.1016/j.tust.2020.103329.

Surarak, C., Likitlersuang, S., Wanatowski, D., Balasubramaniam, A., Oh, E., and Guan, H. (2012). "Stiffness and Strength Parameters for Hardening Soil Model of Soft and Stiff Bangkok Clays." *Soils and Foundations*, 52(4), 682-697. https://doi.org/10.1016/j.sandf. 2012.07.009.

Tanapalungkorn, W., Mase, L. Z., Latcharote, P., and Likitlersuang, S. (2020). "Verification of Attenuation Models Based on Strong Ground Motion Data in Northern Thailand." *Soil Dynamics and Earthquake Engineering*, 133, 106-145. https://doi.org/10.1016/j.soildyn.2020.106145.

Tsinidis, G., de Silva, F., Anastasopoulos, I., Bilotta, E., Bobet, A., Hashash, Y. M., He, C., Kampas, G., Knappett, J., and Madabhushi, G. (2020). "Seismic Behaviour of Tunnels: From Experiments to Analysis." *Tunnelling Underground Space Technology*, 99, 103-334. https://doi.org/10.1016/j.tust.2020.103334.

Vermeer, P., and Brinkgreve, R. (1993). "Plaxis Version 5 Manual." Rotterdam, the Netherlands: *AA Balkema*.

Wang, J.-N. and Munfakh, G. (2001). "Seismic Design of Tunnels." *WIT Press*.

Wang, J. (1993). "Seismic Design of Tunnels: A State-of-the-Art Approach." New York, USA: *Parsons Brinckerhoff Inc.*

Wikipedia (2023). "Algiers Metro." Available at: https://en.wikipedia.org/wiki/Algiers_Metro (Accessed: 26 September 2022).

Wilun, Z., and Starzewski, K. (1972). "Soil Mechanics in Foundation Engineering." New York: *Wiley*.

Zhang, S., Yang, Y., Yuan, Y., Li, C., and Qiu, J. (2022). "Experimental Investigation of Seismic Performance of Shield Tunnel under Near-Field Ground Motion." *Structures*, 43, 1407-1421. https://doi.org/10.1016/j.istruc.2022.07.045.